A Simulated Climatology of Asian Dust Aerosol and Its Trans-Pacific Transport. Part II: Interannual Variability and Climate Connections

S. L. GONG,* X. Y. ZHANG,+ T. L. ZHAO,# X. B. ZHANG,@ L. A. BARRIE,& I. G. MCKENDRY,** AND C. S. ZHAO++

*Air Quality Research Branch, Meteorological Service of Canada, Toronto, Ontario, Canada, and Institute of Earth Environment, Chinese Academy of Sciences, Xian, China

+ Centre for Atmosphere Watch and Services, Chinese Academy of Meteorological Sciences, China Meteorological Administration, Beijing, and Institute of Earth Environment, Chinese Academy of Sciences, Xian, China

Air Quality Research Branch, Meteorological Service of Canada, Toronto, Ontario, Canada, and Centre for Atmosphere Watch and Services, Chinese Academy of Meteorological Sciences, China Meteorological Administration, Beijing, China

@ Climate Research Branch, Meteorological Service of Canada, Toronto, Ontario, Canada

& Air Quality Research Branch, Meteorological Service of Canada, Toronto, Ontario, Canada, and Environment Division, Atmospheric Research and Environment Program, World Meteorological Organization, Geneva, Switzerland

** Atmospheric Science Programme/Geography, University of British Columbia, Vancouver, British Columbia, Canada

++ Department of Atmospheric Science, School of Physics, Peking University, Beijing, China

(Manuscript received 29 March 2004, in final form 30 March 2005)

ABSTRACT

A 44-yr climatology of spring Asian dust aerosol emission, column loading, deposition, trans-Pacific transport routes, and budgets during 1960–2003 was simulated with the Northern Aerosol Regional Climate Model (NARCM). Interannual variability in these Asian dust aerosol properties simulated by the model and its climate connections are analyzed with major climatic indices and records in ground observations. For dust production from most of the source regions, the strongest correlations were with the surface wind speed in the source region and the area and intensity indices of the Asian polar vortex (AIAPV and IIAPV, respectively). Dust emission was negatively correlated with precipitation and surface temperatures in spring. The strength of the East Asian monsoon was not found to be directly related to dust production but rather with the transport of dust from the Asian subcontinent. The interannual variability of dust loading and deposition showed similar relations with various climate indices. The correlation of Asian dust loading and deposition with the western Pacific (WP) pattern and Atmospheric Circulation Index (ACI) exhibited contrasting meridional and zonal distributions. AIAPV and IIAPV were strongly correlated with the midlatitude zonal distribution of dust loading and deposition over the Asian subcontinent and the North Pacific. The Pacific–North American (PNA) pattern and Southern Oscillation index (SOI) displayed an opposite correlation pattern of dust loading and deposition in the eastern Pacific, while SOI correlated significantly with dust loading over eastern China and northeast Asia. The Pacific decadal oscillation (PDO) was linked to variations of dust aerosol and deposition not only in the area of the eastern North Pacific and North America but also in the Asian dust source regions. The anomalies of transport flux and its divergence as well as dust column loading were also identified for eight typical El Niño and eight La Niña years. A shift of the trans-Pacific transport path to the north was found for El Niño years, which resulted in less dust storms and dust loading in China. In El Niño years the deserts in Mongolia and western north China closer to the polar cold air regions contributed more dust aerosol in the troposphere, while in La Niña years the deserts in central and eastern north China far from polar cold regions provided more dust aerosol in the troposphere. On the basis of the variability of Asian dust aerosol budgets, the ratio of inflow to North America to the outflow from Asia was found to be correlated negatively with the PNA index and positively with the WP index.

Corresponding author address: Dr. S. L. Gong, Air Quality Research Branch, Meteorological Service of Canada, 4905 Dufferin Street, Toronto, Ontario M3H 5T4, Canada.
E-mail: sunling.gong@ec.gc.ca

1. Introduction

The production and transport of soil dust has been occurring for at least 2.6 Ma (Liu 1985) as a natural phenomenon in East Asia and was responsible for the formation of the Loess Plateau especially along the valley of the Yellow River in northwest China. During this period, desert areas were regulated by precipitation patterns and climatic variability associated with glacial and interglacial periods (Zhang et al. 1999). Research on Chinese loess deposition shows that millennial-scale rapid variations in dust transport associated with changes in the Asian winter monsoon circulation and source aridity existed during the last glacial (Porter and An 1995) and last interglacial (An and Porter 1997). Extending the present-day dust aerosol observations to the last two glacial cycles, Zhang et al. (2002) found that dust input to the Loess Plateau was high during glacial periods (80–130 μg m^{-3}) and low during interglacial (50–70 μg m^{-3}). This pattern was associated with millennial-scale rapid oscillations in the Asian winter monsoon climate mostly during glacial periods. The existing high glacial dust concentrations could either trigger or modulate rapid variations of winter monsoon climate. Clearly, variability in soil dust aerosol is linked to the variability in climate at long time scales.

In the last 100 years or so, industrialization and population expansion have created another potential source of dust due to the deterioration of ecosystems on the peripheries of natural deserts. These areas are generally known as the anthropogenic deserts. Areas with vegetation cover sustained by a natural precipitation are undergoing desertification processes that have increased desert areas by ~2% to ~7% (Zhong 1999; Zhu and Zhu 1999) in China over the last 40 yr. Furthermore, a recent analysis of Chinese desertification in different time periods (Gong et al. 2003a; Zhang et al. 2003) has placed even more areas with soil dust production potential under the desertification category. However, a 44-yr simulation study of Asian soil dust production with a dynamic desert distribution from 1960 to 2003 suggests that climatic variations play a greater role in explaining the declining trends in dust emission and storm frequencies than desertification processes (Zhang et al. 2003; Zhao et al. 2004; Zhou and Zhang 2003).

In Zhao et al. (2006, hereafter Part I), the mean climate of soil dust aerosols in Asia and their transport over the North Pacific has been characterized through a 44-yr simulation validated with ground and Total Ozone Mapping Spectrometer (TOMS) Aerosol Index (AI) observations. Significant interannual variability was found in both the simulations and observations. A recent effort to correlate a 22-yr model simulation of global mineral aerosols has found a relationship between climate indices and dust (Mahowald et al. 2003) for a number of stations. Dust concentration variability appears to be dominated by transport variability and/or transport and source covariance rather than source strength variability. By analyzing the relationship between climatic factors and the dust storm frequency in Inner Mongolia, China, Zhao et al. (2004) concluded that the intensity and area indices characterizing large-scale cold air mass influence (such as the number of days with gales, and Northern Hemispheric polar vortex and Asian polar vortex indices) controlled dust frequency distributions. This seems to suggest that the variability in the dust source strength is not a major cause of the observed dust concentration variability in the region very close to dust sources. Dust observations in Mongolia during the last 40 yr also showed considerable interannual variability (Natsagdorj et al. 2003). Analyzing the spatial distributions of spring sand/dust storms observed in China and their relationship with atmospheric general circulation, Li and Zhai (2003) found that positive anomalies of the 500-hPa heights over Mt. Ural and negative anomalies over Siberia and Mongolia during spring and the previous winter are associated with highest frequencies of spring sand/dust storms. Negative anomalies over Mt. Ural and positive anomalies over Europe, Siberia, and Mongolia are coupled with the lowest frequencies. Based on the same set of storm data, Qian et al. (2002) investigated the variability of the dust storm and its climatic control by analyzing the 850-hPa geopotential heights and 1000-hPa air temperature from 1949 to 1999. Low air temperature in the prior winter and high-frequency cyclone activity in the spring are strongly positively correlated with the frequency of dust storms in China.

The above-cited research either lacks the spatial coverage (e.g., China only or several points) or uses only surface concentrations or visibility data for climate correlations. Dust production, loading, transport, and deposition were not analyzed. In Part I of this study, modeling and observational results were used to investigate the mean climate of spring Asian dust aerosol emission, concentrations, column loading, deposition, trans-Pacific transport routes, and budgets during 1960–2003 (Part I). These rich data also permit more detailed analysis of the major climate factors influencing the variability of the Asian dust aerosol in East Asia and its trans-Pacific transport to North America. The purpose of this paper is to identify relationships of standard climate indices (including ENSO and PDO), teleconnection patterns and the East Asian monsoon with the interannual variability of Asian dust aerosol and its trans-Pacific transport.

2. Model description and climate data

a. Model

The model [Northern Aerosol Regional Climate Model (NARCM)] used in this study has been used extensively in simulating the dust storms during the Aerosol Characterization Experiment-Asia (ACE-Asia; Gong et al. 2003a). An atmospheric aerosol algorithm—the Canadian Aerosol Module (CAM)—incorporating various aerosol processes including soil dust dry and wet deposition (Gong et al. 2003b) provides the aerosol kernel incorporated in the Canadian Regional Climate Model (RCM), which forms the NARCM. RCM provides the tracer transport and the necessary meteorology within the model domain to drive the aerosol scheme and includes the wind fields, precipitation, soil moisture, and others. In CAM a size-segregated soil dust emission scheme (Alfaro and Gomes 2001; Alfaro et al. 1997; Marticorena and Bergametti 1995) considering that the main mechanisms of saltation bombardment and aggregate disintegration for dust emission are controlled by two parameters: 1) surface wind speed and 2) soil surface properties such as soil texture, fraction of vegetation cover, soil moisture, and snow cover is modified based on the Asian dust measurements, and appropriate input data for Chinese deserts including soil texture and desert distribution maps were used. NARCM runs on a stereographic projection with a horizontal resolution of 100 km at 60°N and 22 vertical levels on a Gal–Chen terrain-following coordinate system from the ground to about 30 km. This model domain covered the Northern Hemispheric regions from East Asia to the North Pacific to western North America (Gong et al. 2003a). The modeling results to date show good agreement with the soil dust strength and frequency in China as well as downwind transport to North America in 2001 (Gong et al. 2003a).

For this study, a 44-yr simulation of every spring from February to May was carried out using the National Centers for Environmental Prediction (NCEP) reanalyzed meteorology as the lateral boundary conditions with surface wind nudged every 6 h. This ensures a realistic dust emission force and transport. The simulation results for March, April, and May are analyzed for climatology of Asian dust aerosol and trans-Pacific transport.

b. Analysis method and data

1) METHOD

To study the climate connections to the 44-yr simulation results from NARCM, a number of observational data and climatic indices were chosen for analysis. The model predictions of dust emission fluxes, column loading, deposition, and dust transport fluxes for the last 44 yr for each grid were correlated with several climatic indices as well as ground observations. Using this approach, spatial distributions of the correlation pattern were obtained. The correlation intervals of $|r| > 0.246$, 0.297, and 0.385 were used in this study to define the significance levels of 90%, 95% and 99%, respectively.

2) OBSERVATIONAL DATA

For the investigation of the influence of precipitation and surface condition on dust emission, the climate data records of precipitation and surface temperature for the period 1960–2001 were compiled from 270 meteorological stations located within 50 km of desert regions in China. In addition to the Chinese climate data records and the republished results, sea level pressure (SLP), 500-hPa geopotential height, and surface and 500-hPa winds from NCEP–National Center for Atmospheric Research (NCAR) reanalysis were used to produce some climate indices.

3) CLIMATE INDICES

(i) East Asian Monsoon Intensity index

To analyze the effect of the East Asian monsoon on Asian dust and its trans-Pacific transport, the East Asian Monsoon Intensity (EAMI) index (Guo 1988; Shi et al. 1996) was used to characterize the strength of the East Asian monsoon. The EAMI index is defined as the sum of the standardized SLP difference at 110° and 160°E over the region from 20° to 50°N. The EAMI index indicates average SLP differences between the East Asian subcontinent (110°E) and northwest Pacific Ocean (160°E). The EAMI index has opposite characteristics for the winter monsoon (EAMI > 0) and summer monsoon (EAMI < 0). During the winter monsoon season (December–May), a cold high dominates the continent where the SLP is higher than that in the northwest Pacific Ocean (positive EAMI). In contrast, for the East Asian summer monsoon season of June to November, a warm low pressure cell prevails over the continent with high pressure over the northwest Pacific (negative EAMI).

(ii) Asian polar vortex and Atmospheric Circulation index in the North Pacific

Data for the area index of the Asian polar vortex (AIAPV) as well as its intensity index of the Asian polar vortex (IIAPV) were taken from Chinese climate data records (Zhao et al. 2004). AIAPV is the area north of the southern boundary of the polar vortex

from 60° to 150°E in Asia. The southern boundary of the polar vortex is the typical isopotential line nearest to the westerly jet at the monthly averaged 500-hPa geopotential surface. The climatological values of the isopotential line are 552, 552, and 560 hPa in March, April, and May. The air mass between the typical isopotential line and the monthly mean 500-hPa geopotential heights north of the southern boundary of the polar vortex from 60° to 150°E in Asia is defined as the IIAPV.

The Atmospheric Circulation index (ACI; King et al. 1998) is a measure of the extent of Rossby wave activity in the midlatitudes. It varies between a "high (zonal) index" indicating a predominance of westerly flow and a "low (meridional) index" indicating a well-developed wave activity and a north–south flow. As such it provides a measure of airmass transport. For trans-Pacific transport of Asian dust aerosol, an ACI in the North Pacific was developed using the averaged zonal wind speed at 500 hPa over the North Pacific region from 30°–55°N to 125°E–140°W.

(iii) Standard indices: WP, PNA EU, SOI, PDO, AO, and ENSO

The atmospheric teleconnection patterns of the western Pacific (WP), Pacific–North America (PNA), and Eurasia (EU), as originally identified by Wallace and Gutzler and subsequently corrected (Barnston and Livezey 1987; Wallace and Gutzler 1981), are used for the winter season. The Southern Oscillation index (SOI) describes an east–west atmospheric pressure seesaw in the tropical Pacific (Webster 1987). The PDO index is derived as the leading principal component of monthly SST anomalies in the North Pacific Ocean, poleward of 20°N. The monthly mean global average SST anomalies are removed to separate this pattern of variability from any "global warming" signal that may be present in the data (Mantua et al. 1997; Y. Zhang et al. 1997). The Arctic Oscillation (AO) data were based on the expansion coefficient time series of the pattern of surface air temperature anomalies associated with the AO (Thompson and Wallance 1998). (The climate indices of WP, PNA EU, SOI, and AO are available online at http://www.cdc.noaa.gov/ClimateIndices/.)

El Niño–Southern Oscillation (ENSO) represents a coupling between atmosphere and ocean in the tropical pacific. Based on the multivariate ENSO index (MEI; Wolter and Timlin 1998) from 1960 to 2003, 1966, 1969, 1973, 1983, 1987, 1992, 1998, and 2003 were classified as typical El Niño years and 1965, 1971, 1974, 1976, 1986, 1989, 1999, and 2000 as typical La Niña years in the composite maps used below to discuss the relationship of Asian dust aerosol with the ENSO.

Table 1 summarizes the above-mentioned climatic indices and corresponding typical variations of atmospheric circulation. It may be used in the following section as an aid to the physical interpretation of correlation of Asian dust aerosol with the various indices.

3. Asian dust variability and climate connections

The various climate indices were correlated with soil dust emission, loading, dry/wet deposition, transport, and budgets. As each climate index has an influence on these processes, the results for each process are presented separately.

a. Dust emission strength

The correlations of Asian dust emission with (a) surface wind speed and (b) the simulated precipitation over the dust source regions in spring from 1960 to 2003 are shown in Fig. 1. Dust source strength and its interannual variability in Asia has been published for 10 major dust source regions (Zhang et al. 2003). The distribution of the 10 major dust source regions is indicated in Fig. 2. As the driving force for dust mobilization, the accumulated surface wind speed in source regions is strongly correlated with the 44-yr simulation of the surface flux (Fig. 1a). The inset scatterplot indicates a correlation coefficient of 0.58. The sensitivity of the dust emission in each region to the variations of the major climate indices—APV, SOI, WP, EU, PNA, AO, PDO, and EAMI—is also presented in Table 2. Significant correlations exceeding the 90% level for each region are shaded, while the negative correlations are italic. For most major northern and northwestern sources of Asian dust (S2, S4, S5, and somewhat in S6; Fig. 2), the intensity of APV correlates positively with the dust emission strength, showing that most Asian dust storms were derived from the north and northwestern sources when APV was well developed. This is also supported by the negative correlation between intensity of APV and dust emission strength from northeastern sources of Asian dust (S8 and S7, in Fig. 2). The area indices of APV showed similar trends. Defined as the area and intensity of the Asian polar vertex, the AIAPV and IIAPV reflect the strength and area of the cold frontal systems. These are strongly correlated with surface wind speeds (Fig. 2) in most source regions, except the sources in northeastern China (S8 and S9) and a minor source (S10). These results again indicate that surface accumulated wind speed is one of the dominating factors controlling the occurrence of Asian dust storms, especially those occurring in northern and northwestern regions.

TABLE 1. Climatic indices and corresponding typical atmospheric circulation.

Indices	Positive	Negative
SOI	La Niña events and strong convection in the tropical western Pacific	El Niño events and weak convection in the tropical western Pacific
WP	The westerly trough with the entrance region of the jet stream located in the East Asian continent	The westerly trough with the entrance region of the jet stream located near Japan in the western Pacific
EU	The meridional midlatitude circulation over large portions of Europe and Asia with a positive height anomaly center over Mt. Ural and separate centers of opposite sign to the polar anomaly over Europe and northeastern China	The zonal midlatitude circulation over large portions of Europe and Asia with a negative height anomaly center over Mt. Ural and separate centers of opposite sign to the polar anomaly over Europe and northeastern China
PNA	Strong westerly jet in the eastern Pacific and meridional circulation from the eastern Pacific to North America	Weak westerly jet in the eastern Pacific and zonal circulation from the eastern Pacific to North America
AO	Positive 1000-hPa height anomalies poleward of 20°N	Negative 1000-hPa height anomalies poleward of 20°N
EAMI	East Asian winter monsoon	East Asian summer monsoon
PDO	Positive monthly SST anomalies in the North Pacific Ocean, poleward of 20°N	Negative monthly SST anomalies in the North Pacific Ocean, poleward of 20°N
	High	Low
AIAPV	Large area around the north polar vortex north of the westerly jet at 500 hPa from 60° to 150°E that accompanies the zonal circulation pattern in Asia and the western Pacific	Small large area around the north polar vortex north of the westerly jet at 500 hPa from 60° to 150°E that accompanies the meridional circulation pattern in Asia and the western Pacific
IIAPV	Strong westerly jet from 60° and 150°E that reflects intensive cold frontal activity with gales over East Asia and strong trans-Pacific transport	Weak westerly jet from 60° and 150°E that reflects decreased cold frontal activity with gales over East Asia and weak trans-Pacific transport
ACI	Predominance of zonal flow in the troposphere over the North Pacific	Predominance of meridional flow in the troposphere over the North Pacific

In addition to surface wind speed, soil moisture has a major impact on dust emission (Gong et al. 2003a). In the absence of soil moisture data, records of two related parameters, precipitation and soil temperature, were correlated with modeled dust emissions. Table 3 shows the coefficients of correlation for three groups of deserts (defined in Table 2) in northern China for both precipitation and surface temperature. Simulated dust emissions were negatively correlated with the observed precipitation around all desert groups for the current spring (March–May) and the previous winter (December–February). Similar correlations between dust emission and model-predicted precipitation in all Asian deserts of the model domain were also obtained in Fig. 1b, which shows the interannual variation of the Asian dust emission and the modeled precipitation over Asian deserts in spring. The inset scatterplot shows a correlation coefficient of -0.48. The similarity in correlations associated with the observed and modeled precipitation (Table 3 and Fig. 1b) suggests that NARCM produces reasonable interannual variability of precipitation, and hence soil moisture, in the dust source regions. The correlation with the observed temperature has the same trend for western and central deserts but an opposite correlation in the eastern desert in the current spring. It is known that the most favorable atmospheric circulation pattern for Asian dust storms is characterized by cold fronts sweeping across the deserts with cyclones between Mongolia and northeastern China (Chun et al. 2001; Qian et al. 2002). Low temperatures in the western and central desert regions result from the passage of a cold front from the north, while over the eastern deserts of north China, warm air advection from the south associated with the eastern side of the cyclones produces a warm surface air mass. The latter produces a positive correlation between temperature and dust emission in northeastern China.

The East Asian monsoon, driven dominantly by land–sea thermal contrasts between the Asian subcontinent and the western Pacific Ocean, constitutes a major circulation feature in the Northern Hemisphere and may be represented by the EAMI. It is interesting to note that only a weak negative correlation with EAMI (Table 4) was found for most desert regions in the current spring (March–May) and prior winter (December–February). The major positive correlations for the current spring were found for the deserts S7 and S8. According to the definition in section 2b(3), the EAMI has opposite characteristics for the winter monsoon (EAMI > 0) and summer monsoon (EAMI < 0). As the land–sea contrast reverses direction in the summer monsoon season, a more negative EAMI represents a stronger

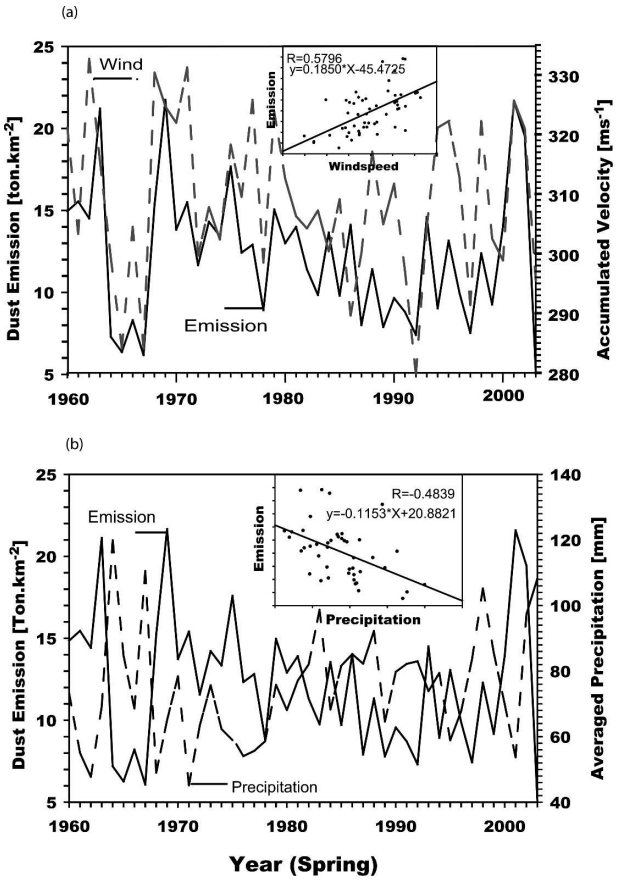

FIG. 1. The correlations of Asian dust emission with (a) surface wind speed and (b) the simulated precipitation over the dust source regions in spring from 1960 to 2003.

summer monsoon. The correlations with EAMI for the prior summer monsoon season should be interpreted reversely, that is, negative values for significant connections (shaded values in Table 4). On this basis it appears that dust emission is also enhanced somewhat by the prior summer monsoon for most regions, except S7 and S8. The weak correlations seem contradictory to previous research indicating that the East Asian monsoon drives dust aerosol from the desert regions in East Asia (Merrill et al. 1989). However, a careful examination of the EAMI suggests that the index may be more appropriate in analyzing the trend of dust transport off the Asian continent than controlling dust emission. According to the monsoon definition from Ramage (1971), most deserts in Mongolia and northwestern China are not located in the East Asian monsoon region. The uplift and extent of the Himalaya–Tibetan Plateau caused the evolution of the western arid regions and the eastern monsoon regions in the East Asian subcontinent (An et al. 2001). The EAMI describes only the strength of the cold surge from the continent to the Pacific in the East Asian monsoon region but not the southward invasion of polar cold air with high surface winds over Mongolia and northwestern China in the arid regions. During the winter monsoon season, a cold high dominates the East Asian monsoon region over the continent (positive EAMI). A high EAMI characterized by a strong and/or persistent cold high over the East Asian subcontinent reduces the pressure difference between high latitudes and the East Asian monsoon region over the subconti-

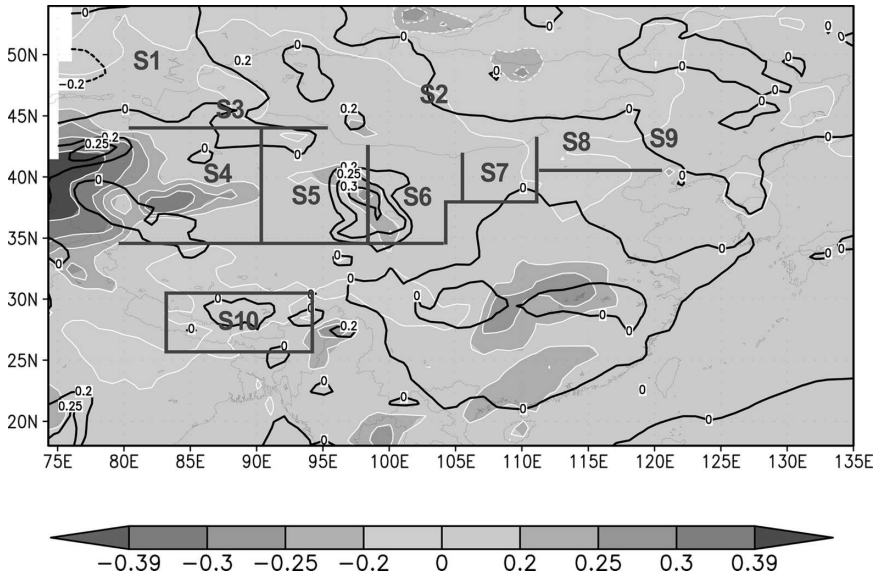

FIG. 2. The correlations of the surface wind speed with AIAPV and IIAPV (contour lines). The geographical distribution of Asian deserts is shown with 10 regions from S1 to S10.

TABLE 2. The correlations of Asian dust emission in spring with the climatic indices. Deserts within China are grouped into western, central, and eastern regions. Desert regions S1 to S10 are defined in Fig. 2

Asian desert region		APV		SOI	WP	EU	PNA	AO	PDO	EAMI
		Intensity	Area							
	S1	0.201	0.146	0.135	−0.208	0.045	−0.041	−0.081	−0.117	−0.242
	S2	0.382	0.274	0.221	0.060	0.079	−0.070	−0.116	*−0.345*	−0.045
Western	S3	0.013	−0.022	0.149	−0.147	0.143	−0.141	−0.077	−0.058	*−0.278*
	S4	0.512	0.094	0.148	*−0.361*	0.203	−0.066	0.034	−0.115	−0.248
	S5	0.287	0.077	−0.115	*−0.287*	0.121	0.181	0.216	0.146	−0.082
Central	S6	0.150	0.418	0.321	0.048	0.087	0.066	−0.044	−0.073	0.067
	S7	−0.131	0.163	−0.041	−0.066	−0.044	0.278	0.138	0.251	0.241
Eastern	S8	−0.243	0.047	−0.114	0.102	−0.093	0.021	0.035	0.167	0.193
	S9	0.074	0.072	−0.089	0.107	0.062	0.184	−0.041	0.212	−0.009
	S10	−0.001	0.095	0.378	0.107	0.016	−0.196	−0.219	*−0.367*	0.030

nent. Consequently, this inhibits the passage of cold fronts and lowers surface winds that are responsible for dust emission for most East Asian deserts. This is reflected in negative correlations for the most deserts with positive correlations for the Chinese eastern deserts near the western Pacific and in the zone of cold surges of Asian winter monsoon from the continent to ocean. Furthermore, the correlation between dust emission and EAMI for the prior winter was stronger than the current spring for most regions (Table 4). This suggests that EAMI is more important in regulating the long-term surface conditions of source regions via interannual anomalies of atmospheric circulation than controlling the current emission potential. Additionally, in view of millennial-scale variations and the fact that the present day is part of an interglacial period associated generally with a warm and humid climate background, the weak correlation, especially in northwestern sources, is also consistent with two previous studies on the long-term loess record (X. Y. Zhang et al. 1997; Zhang et al. 2002). In those studies, Asian dust was found to have a minor relationship with the variation of land–ocean thermal contrast and winter monsoon system during interglacial when the summer monsoon prevails (Zhang et al. 2002).

It should be pointed out that the 44-yr simulations have taken desertification into consideration. As our previous research indicated, climate variability has had a greater impact than the desertification process in controlling the occurrence of dust storms in East Asia (Zhang et al. 2003). This analysis further confirms that the major governing climate indices that regulate dust emission are the surface winds, the intensity, and area of APV. APV directly affects the magnitude and frequency of polar cold air outbreaks in Asia. These polar cold air outbreaks intensify the Asian winter monsoon because of the southward incursion of cold air masses into the East Asian monsoon region. As a consequence, it is likely that this buildup of a cold high pressure in the East Asian monsoon region will also hamper further polar cold air intrusions that are responsible for strong surface winds over the Asian deserts. Therefore, the strength of the East Asian winter monsoon was not found to be directly linked to the Asian dust emission with respect to interannual variability.

The variations of dust emission over the major sources of Asian dust (S2, S4, and S6) are positively correlated with the SOI (Table 2). The deserts in Mongolia (S2), the Taklimakan Desert (S4) in western China, and the Badain Juran Desert (S6) in northern China (averaged contributions of 29%, 21%, and 22% of the total Asian dust production) dominate Asian dust emission into atmosphere (Zhang et al. 2003). This indicates a reduced frequency of Asian dust storms in El Niño years (negative SOI). It is interesting to note in Table 2 that variation of dust emission, as a result of wind and surface conditions in the southern Tibet source (S10), was most strongly correlated with SOI

TABLE 3. The correlations of dust emissions with the observed precipitation and surface temperature at the stations within 50 km around the desert regions of northern China.

	Current spring (Mar–May)		Prior winter (Dec–Feb)		Prior summer (Jun–Nov)	
	Precipitation	Temperature	Precipitation	Temperature	Precipitation	Temperature
Western	−0.242	−0.168	−0.116	−0.194	−0.286	+0.028
Central	−0.336	−0.358	−0.090	−0.159	+0.095	−0.203
Eastern	−0.222	+0.239	−0.192	−0.029	+0.032	−0.011

TABLE 4. The correlations of Asian dust emission in spring with the EAMI.

Asian desert region	Current spring (Mar–May)	Prior winter (Dec–Feb)	Prior summer half year (Jun–Nov)
S1	−0.242	−0.242	−0.106
S2	−0.045	−0.348	−0.229
S3	−0.278	−0.095	−0.003
S4	−0.248	−0.311	−0.272
S5	−0.082	−0.069	−0.009
S6	0.067	−0.074	−0.021
S7	0.241	0.158	0.264
S8	0.193	0.254	0.111
S9	−0.009	−0.273	−0.088
S10	0.030	0.109	−0.225

($r = 0.38$) and PDO ($r = -0.37$). These correlations suggest that the influence of SST variability in the Pacific extends beyond the western arid regions and the eastern monsoon regions in the East Asian subcontinent to the Himalaya–Tibetan Plateau (Chen et al. 2001; Webster and Yang 1992).

b. Dry/wet deposition and column loading

Once emitted, dust aerosols are transported by atmospheric circulation patterns and are deposited by the removal processes. Asian dust aerosol over the North Pacific is mainly scavenged by precipitation along the trans-Pacific transport path into the ocean (Zhao et al. 2003). As the dust could be transported thousands of kilometers downwind of source regions, the controlling climate factors should be different from those controlling emissions. It has been suggested that the wet to dry ratios of dust emission are a function of distance downwind of source regions and vary from less than 0.1 at sources to more than 20 over the North Pacific (Part I), which is mainly due to the difference in precipitation patterns over the transport paths and dust particle size. The variability of spring deposition and column loading patterns is shown in Fig. 3 as the correlations of the 44-yr simulation results to the corresponding indices of WP, ACI, AIAPV, IIAPV, PNA, SOI, and PDO. The deposition and loading correlations are represented by filled contours and contour lines, respectively.

Among the indices, WP and ACI correlation patterns show complementary spatial distributions, especially in East Asia and the western Pacific (Figs. 3a,b). The WP index reflects pronounced zonal and meridional variations in the location and intensity of the entrance region of the Pacific jet stream associated with the westerly trough (East Asian major trough) at 500 hPa between East Asia and the western Pacific. The typical circulation pattern for positive WP is a westerly trough with the entrance region of the jet stream located close to the deserts in East Asia with a strong meridional airflow. The stronger meridional airflow produces greater dust loading and deposition in the northeast region of the Asian continent and the southwest Pacific portion of the model domain. Reduced trans-Pacific transport is found along the westerly jet over the Pacific around 40°N in positive WP (Fig. 3a). The ACI reflects the predominance of zonal or meridional flow over the North Pacific. Positive ACI, with strong zonal airflows over the North Pacific, favors significant trans-Pacific dust transport from the continent and greater dust loading and deposition over the region from the western North Pacific to the eastern North Pacific and North America (Fig. 3b).

Correlations fields for AIAPV and IIAPV are very similar (Figs. 3c,d). A significant feature of the distributions is the positive correlation between dust deposition and loading over the regions from East Asia to North America between 35° and 45°N, with the most significant IIAPV correlations over Asian deserts and western North America. AIAPV is associated with the area around the North Polar vortex north of the westerly jet at 500 hPa over Asia. High AIAPV reflects the large area that accompanies the zonal circulation pattern in Asia and extending into the North Pacific. Consequently, this produces the zonal AIAPV correlation pattern along the westerly jet (Fig. 3c). The IIAPV is an index of westerly jet intensity in Asia and the western Pacific from 60° to 150°E. A strong westerly jet (high IIAPV) brings intense cold frontal activity with gales over East Asia, producing more dust from the dust sources and strong trans-Pacific transport to North America. This results in more significant IIAPV correlations over the Asian deserts and western North America than for AIAPV correlations (Fig. 3d).

The PNA index reflects the zonal and meridional variations of circulation pattern with the location and intensity of the westerly jet from the East Pacific to North America. It is also directly linked to El Niño and La Niña events, corresponding with a negative and positive SOI. A positive PNA, as a result of a negative SOI, favors dust transport convergence over the East Pacific because of the strong westerly jet there. This relationship was verified in the PNA and SOI correlation pattern especially in the eastern Pacific (Figs. 3e,f). The SOI represents the variability in the Indo-Pacific Walker circulation in the Tropics, and consists of an east–west atmospheric pressure seesaw in the tropical Pacific that directly affects the tropical circulation around the globe (Webster 1987). The variability of the tropical circulation in the western Pacific may excite a

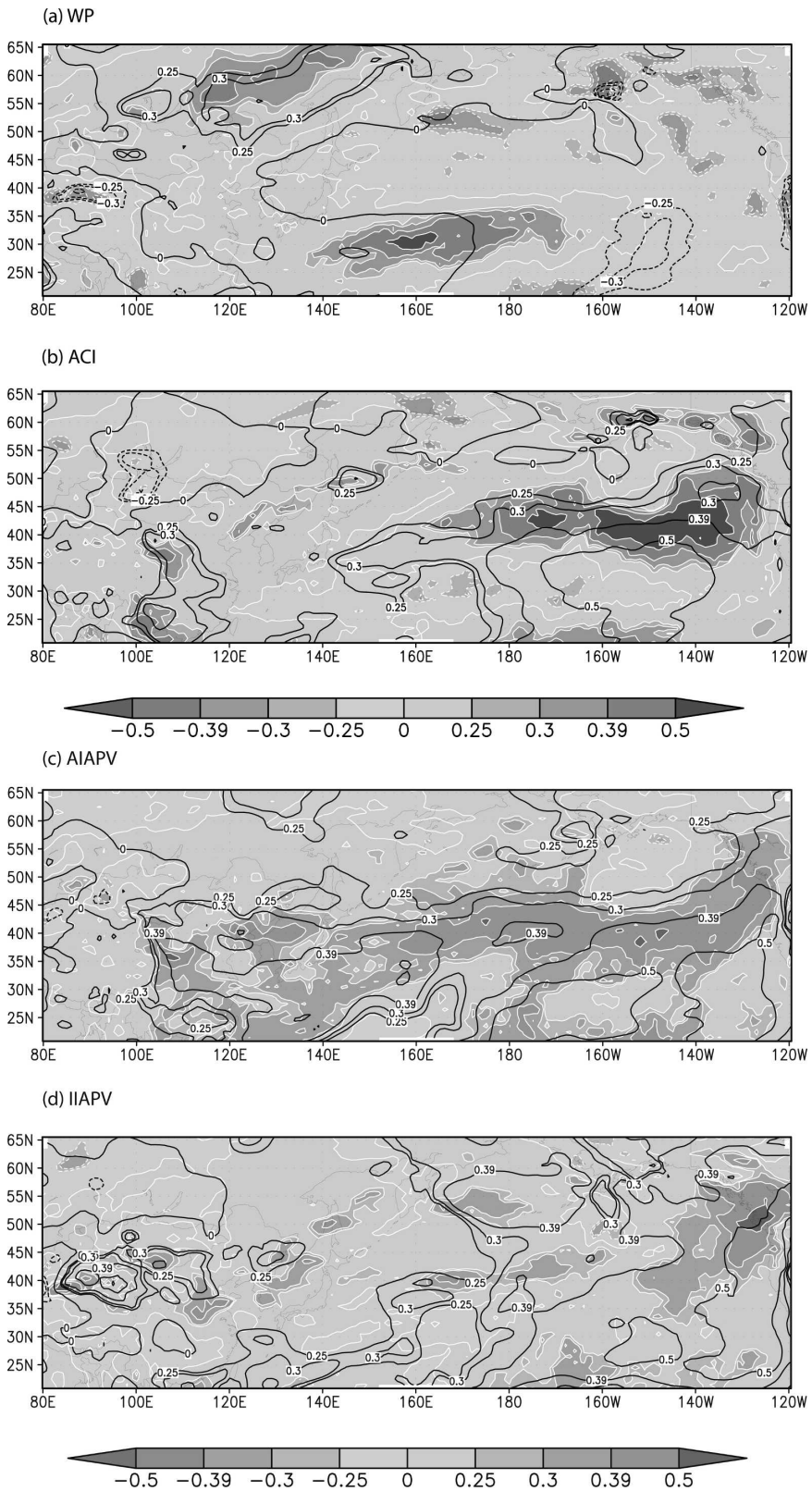

FIG. 3. The correlation patterns of the Asian dust aerosol with the indices of (a) WP, (b) ACI, (c) AIAPV, (d) IIAPV, (e) PNA, (f) SOI, and (g) PDO. The dust deposition and loading correlations are represented by filled contours and contour lines, respectively. The positively and negatively correlated contours are also identified with solid and dashed lines, respectively.

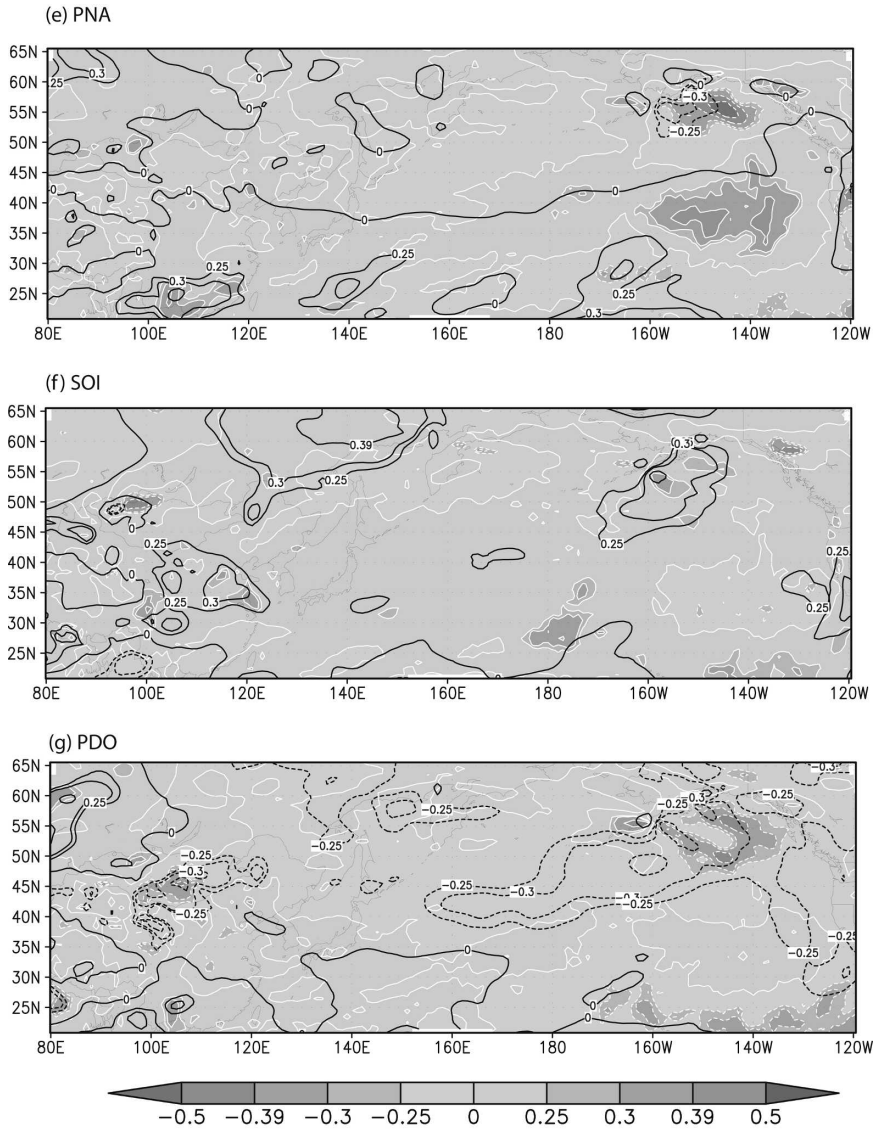

FIG. 3. (*Continued*)

stationary wave train, thus producing a meridional teleconnection pattern [Pacific–Japan (PJ) or East Asia–Pacific (EAP)] over the western Pacific and East Asia (Huang and Li 1988; Nitta 1986). Through this meridional teleconnection pattern, the positive SOI with the enhancement of convective activity in the tropical western Pacific correlates with positive dust loading over eastern China and northeastern Asia (Fig. 3f). This correlation relationship with SOI is characterized by less dust loading in eastern China and northeastern Asia during El Niño years (negative SOI).

Even in the absence of theoretical understanding, Pacific decadal oscillation (PDO) climate information improves season-to-season and year-to-year climate forecasts for North America (Mantua 1999). Figure 3g shows the impacts of PDO on the interannual variability of Asian dust aerosol. During the warm phase of the PDO (positive index), there is less dust aerosol and deposition in the midlatitudes, especially in the area from the eastern North Pacific to North America, as well as in the Asian dust source regions. The widespread nature of this influence is likely due to air–sea interactions between the global westerly belt and SST in the North Pacific.

It is also interesting to note in Fig. 3 that the dust column loading (dashed contour lines) has the same sign as deposition correlations in most regions, indicating that dust deposition is larger where there is more dust loading. However, the deposition centers are located on the north side of the westerly jet where the

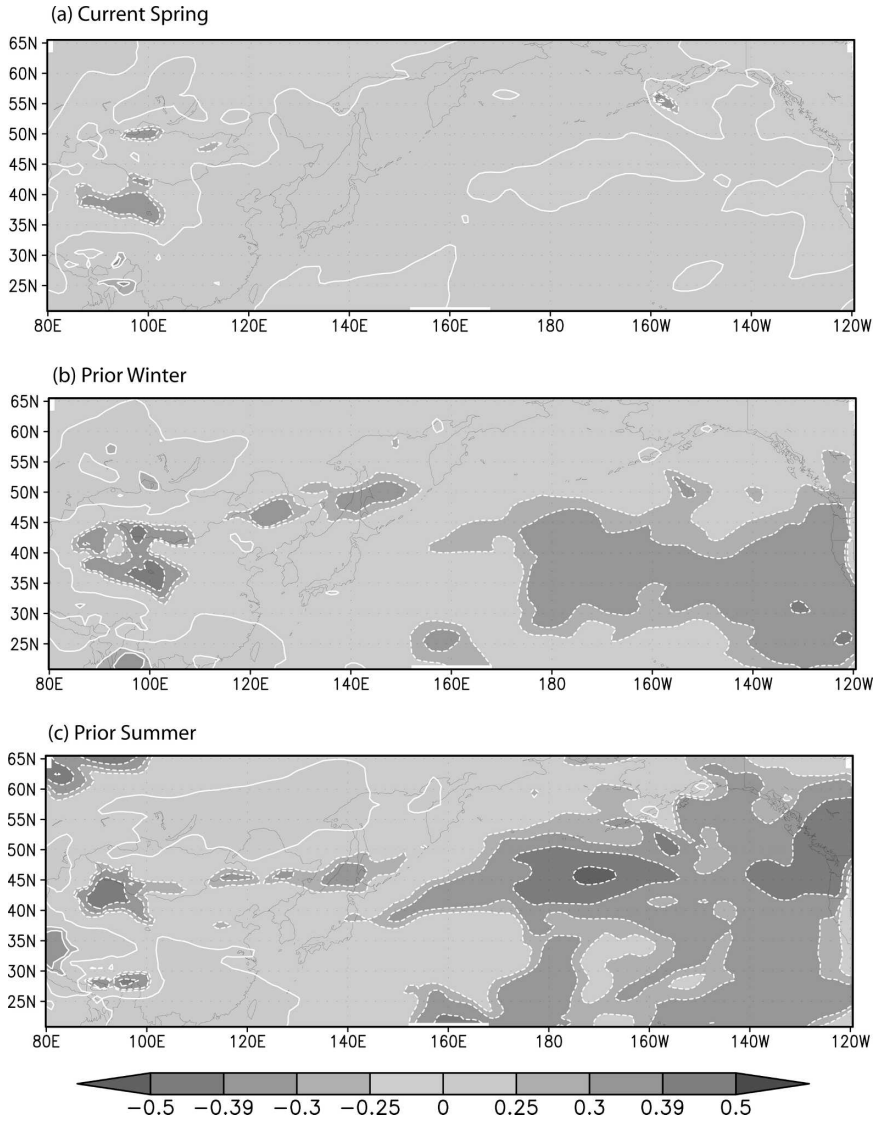

FIG. 4. The correlations of soil dust loading with EAMI for the (a) current spring, (b) prior winter, and (c) prior summer. The positively and negatively correlated contours are also identified with solid and dashed lines, respectively.

cyclonic shear creates major precipitation areas. Asian dust transport along the westerly jet forms the major loading pattern, with the center on the south side, while the deposition is centered on the north side of the westerly jet.

The East Asian monsoon also plays an important role in the global circulation, ENSO, and global climate system at the interannual time scale (An et al. 1990; Ding 1994; Lau and Yang 1994; Yasunari and Seki 1992). In section 3a, it was shown that the EAMI has a rather weak correlation with dust emissions. To further investigate the function of the Asian monsoon in Asian dust aerosols, the correlation of dust loading with EAMI is presented in Fig. 4 for three consecutive seasons: 1) current spring (Fig. 4a), 2) prior winter (Fig. 4b), and 3) prior summer (Fig. 4c). A generally weak and positive correlation ($r < 0.25$) was found for the current spring with highs around Korea and southern Japan, the Sea of Okhotsk, and the middle Pacific. For the prior winter/summer, there are significant negative/positive correlations with EAMI in the east Pacific between 35° and 50°N. These indicate that a low springtime dust loading in the east Pacific followed a stronger East Asian winter monsoon; a stronger summer monsoon (negative correlations) in East Asia was followed by greater springtime dust loading in the east Pacific

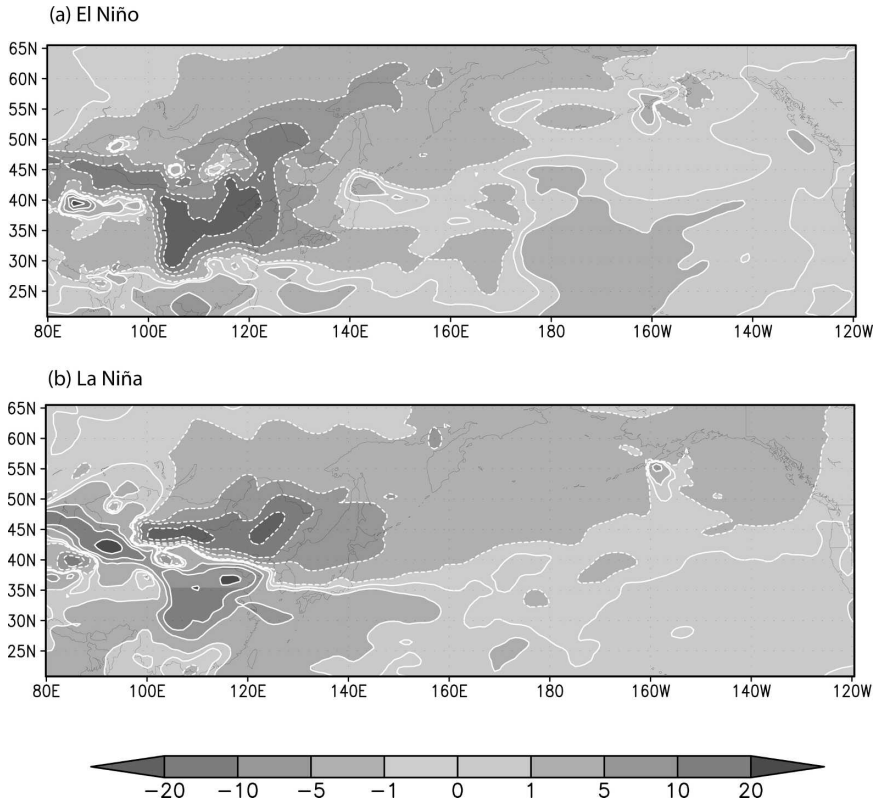

FIG. 5. The anomalies of dust aerosol loading (kg km^{-2}) in (a) eight El Niño years (1966, 1969, 1973, 1983, 1987, 1992, 1998, and 2003) and (b) eight La Niña years (1965, 1971, 1974, 1976, 1986, 1989, 1999, and 2000) relative to the 44-yr mean of Asian dust aerosol in spring. The positively and negatively correlated contours are also identified with solid and dashed lines, respectively.

and western North America. From these connections, it seems to confirm that though the interannual variability of the East Asian monsoon strength has little influence on soil dust emission in Asia, it has a strong impact on the trans-Pacific transport of Asian dust. The interannual variability of the East Asian monsoon also serves to modulate surface conditions on the Asian continent by changing the strength of surface wind speed and precipitation patterns via interannual anomalies of atmospheric circulation.

Finally, the anomalies of dust loading for eight typical El Niño and eight La Niña years from the 44-yr-averaged values are presented in Fig. 5. Contrasting situations were shown in most parts of China with a sharp negative anomaly for El Niño years (Fig. 5a) and a positive anomaly for La Niña years (Fig. 5b). The contrasting band starts from the north of the Taklimakan Desert (45°–50°N, 80°E) and continues down the China–Mongolia border and over most of the Loess Plateau and southwest and central China. ENSO exhibits the greatest impact on the interannual variability of the global climate, especially of the Asian monsoon (Webster et al. 1998). El Niño and La Niña are opposite phases of the ENSO cycle and the strongest climatic signal in the Tropics and can lead the East Asian winter monsoon to be weak (strong) through teleconnections or remote responses (Li et al. 2001; Tomita and Yasunari 1996) and the variability in precipitation and surface conditions over the Asian subcontinent. Consequently, the climate in southeastern China and the surrounding regions in East Asia is warmer and wetter with the weak cold air activity during El Niño or colder and drier with the strong cold airflow during La Niña than normal in the ensuing spring (Kang and Jeong 1996; Tao and Zhang 1998). The anomalies of Asian dust loading in Fig. 5 over those regions accompanied well the anomalies of cold air activity in the El Niño and La Niña years. In western North America, positive anomalies in dust loading occur during El Niño years north of 45°N (with negative anomalies to the south), while during La Niña years the opposite pattern is evident. This north–south "seesaw" pattern has also been documented for precipitation in western North America and has been attributed to southward move-

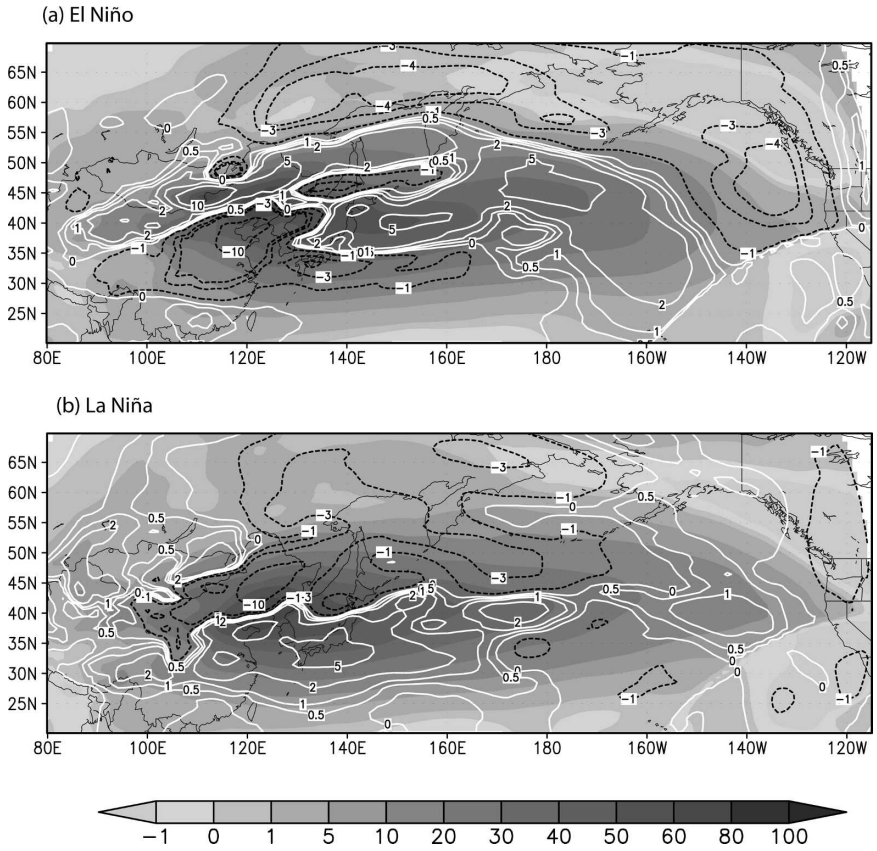

FIG. 6. Same as in Fig. 5, but for the zonal transport fluxes (μg m^{-2} s^{-1}) of Asian dust in spring. The contour lines are for the anomalies relative to the 44-yr mean of Asian dust aerosol in spring.

ment of storm tracks during El Niño years (Cayan et al. 1999; Cayan et al. 1998). A positive anomaly is also evident in the mid-Pacific (160°W–180°) during El Niño years.

Asian dust aerosol contributes most of the dust aerosol loading in the troposphere and dust deposition over the midlatitude regions from East Asia to the North Pacific and western North America during springtime. The interannual variability of Asian dust loading and deposition is modulated by interannual anomalies of atmospheric circulation teleconnection patterns, Asian monsoon, and ENSO. The distributions of the correlation patterns imply that significant correlations of those anomalies with the changes of radiative forcing, atmospheric chemistry, and the sediments in land and ocean may be expected over large areas of the Northern Hemisphere as a result of the interannual variability of Asian dust production and transport.

c. Asian dust transport

ENSO exhibits a remarkable impact on the intensity and position of the westerly jet over the North Pacific, the Asian monsoon, and precipitation and surface conditions over the Asian subcontinent (Wang et al. 2000). These factors are all closely associated with Asian dust production, deposition, and transport. Trans-Pacific transport of soil dust has been shown to be dependent on atmospheric circulation patterns (Zhao et al. 2003). An analysis of the variability of the 44-yr zonal transport flux, that is, concentrations multiplied by westerly/easterly wind speeds, was conducted for eight typical El Niño and eight La Niña years. The zonal transport flux indicates the major transport routes and direction of Asian dust across the Pacific. Most trans-Pacific transport of Asian dust aerosol occurs in the middle troposphere between 3 and 10 km (Part I). Figure 6 shows the averaged dust transport flux (filled contours) for El Niño (Fig. 6a) and La Niña (Fig. 6b) years integrated from 3 to 10 km. On the same plot, their anomalies (dashed contour lines) from the 44-yr-averaged values are also superimposed. The sharp difference between El Niño and La Niña years is the center of the transport path. During El Niño years, trans-Pacific transport is centered at 45°N, while during La Niña years it is

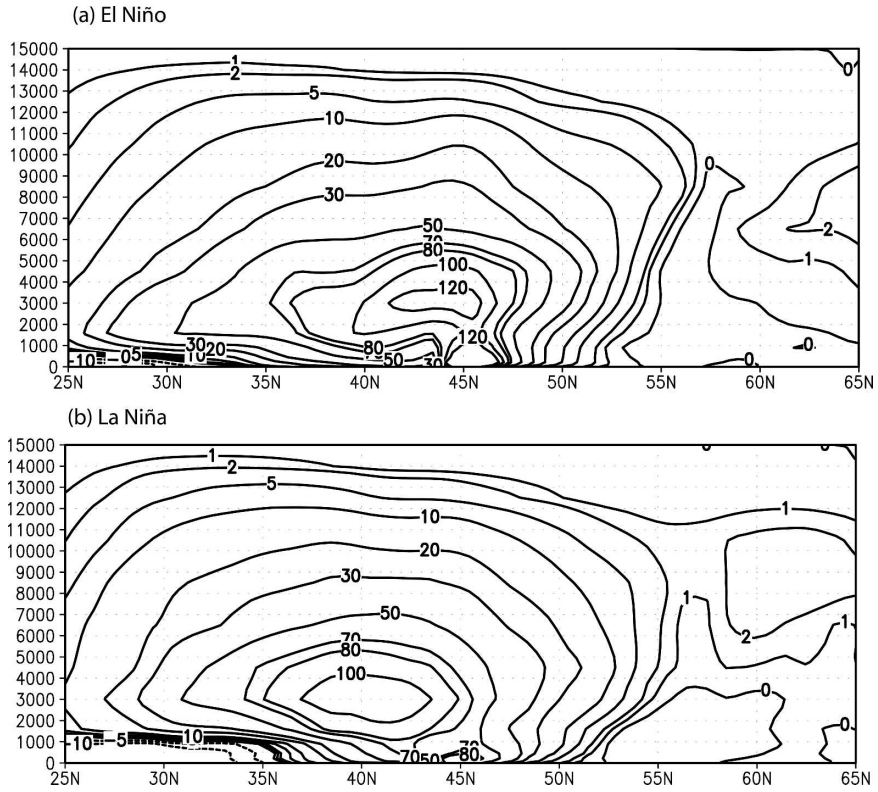

FIG. 7. Same as in Fig. 6, but through 125°E in spring.

around 40°N. The zonal transport fluxes of Asian dust aerosol through 125°E in spring for the same El Niño (Fig. 7a) and La Niña (Fig. 7b) years indicate a shift of the outflow point in Asia from 45° to 40°N during La Niña years. In contrast, in the eastern Pacific (Fig. 8; 140°W) and entering the coast of North America, peak transport moves southward from 45° to 40°N during El Niño years and to lower heights (5000 m during El Niño versus 6500 m during La Niña years).

To examine the impact of ENSO on the regional transport of Asian dust in East Asia, the anomalies of averaged flux transport divergence in both the zonal and meridional direction in the troposphere below 3 km (Fig. 9) and between 3 and 10 km (Fig. 10) were analyzed for El Niño and La Niña years. The interesting feature of those anomaly patterns is that the anomalies reverse between El Niño and La Niña years in most regions of East Asia. The El Niño and La Niña, the two opposite phases of the ENSO cycle in the tropical Pacific, may cause an anomalously weak (strong) East Asian polar front over the Asian subcontinent and western North Pacific (Wang et al. 2000) in the spring. In Figs. 9 and 10 the positive (negative) anomalies of dust flux divergences represent the stronger (weaker) dust contributor in the atmosphere. In El Niño years, the anomalously weak East Asian polar front most likely affected the deserts closer to the polar cold air regions in Mongolia and western north China where the deserts contributed more dust aerosol in the troposphere, while in La Niña years the deserts in central and eastern north China far from polar cold regions provided more dust aerosol in the troposphere, as cold airflow could reach these desert areas with the anomalously strong East Asian polar front. ENSO caused an obvious anomaly in the regional transport pattern of Asian dust, the exports to the long-range transport, and the contributions of Asian dust aerosol from the different desert source regions to the transport of Asian dust aerosol.

A comprehensive picture of soil dust budgets and their interannual variability over source regions and the North Pacific is needed to fully understand the characteristics of soil dust and future climate impacts. A detailed description of the budgets has been given in Part I. The analysis in this paper has focused on the climate connections of the following quantities: 1) deposition in Asian subcontinent, 2) outflow from the Asian continent, 3) deposition over the North Pacific, and 4) inflow to North American continent. Table 5 lists the correlation coefficients of nine climate indices to the total dust

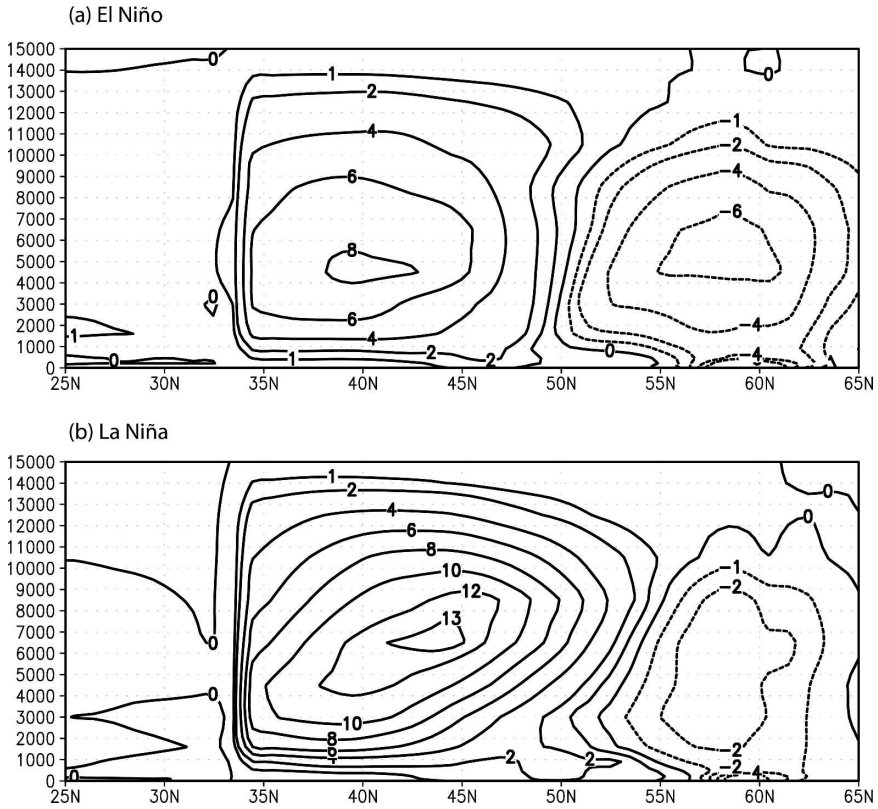

FIG. 8. Same as in Fig. 6, but through 140°W in spring.

depositions in the Asian subcontinent and North Pacific and to the ratio of in- and outflow of dust over the North Pacific. The latter quantity is a measure of relative mass that was transported into the North American continent. The maximal positive (negative) correlations among nine climate indices in Table 5 are shaded (italic). Not surprisingly, deposition over deserts and nondeserts over the Asian subcontinent as well as over the North Pacific are all correlated with IIAPV over the 44 simulation years. The deposition over the North Pacific is, however, positively connected with ACI and negatively with WP. Those relationships of deposition over desert and nondesert regions in the Asian subcontinent as well as over the North Pacific with the IIAPV, ACI, and WP are consistent with the correlation patterns of Asian dust deposition in Fig. 3.

Another quantity that characterizes the Asian long-range transport and input to North America is the ratio of inflow to North America to the outflow from the Asian continent to the North Pacific. It reflects the relative amounts of dust that reach the North American continent to those that enter the Pacific from Asia. From Table 5, it is shown that this ratio was positively correlated with WP and negatively with PNA. As discussed above, a positive WP or PNA represented an enhanced meridional circulation pattern between the Asian subcontinent and western Pacific or between the eastern Pacific to North America. Less dust exported from the Asian continent (outflow) corresponds to a larger ratio with a positive WP, while more dust imported from the eastern Pacific to North America (inflow) corresponds to a larger ratio as well as a negative PNA. A positive PDO brought decreasing dust deposition in the East Asian subcontinent and North Pacific as well decreased Asian dust transport to North America.

4. Conclusions

The interannual variability of spring Asian dust aerosol and trans-Pacific transport as well its climate connections have been analyzed from the results of a 44-yr simulation and ground climatic records since 1960. The major conclusions may be summarized as follows.

1) The production of spring Asian dust aerosols is strongly correlated with the surface wind speed in the source regions, and the area (AIAPV) and intensity (IIAPV) indices of the Asian polar vortex. Asian dust emission from the major source regions is reduced in El Niño years (negative SOI). The variation of dust emission from the southern Ti-

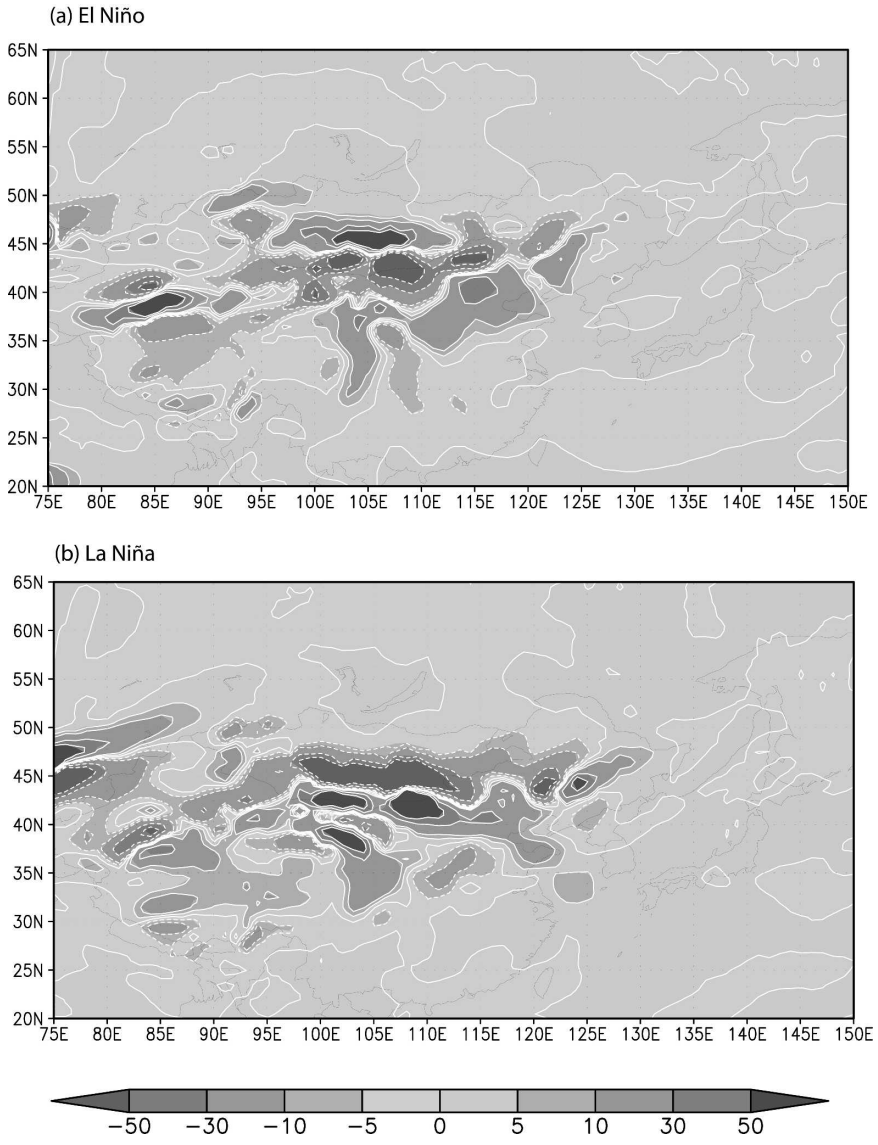

FIG. 9. Same as in Fig. 5, but for Asian dust transport flux divergence ($\times 10^{-05}$ μg m^{-3} s^{-1}) below 3 km in spring.

betan source was significantly correlated with SOI and anticorrelated with PDO.

2) The strength of the East Asian monsoon was not found to be directly linked to dust production but rather to the modulation of the surface conditions and outflow of dust from the Asian subcontinent via interannual anomalies of atmospheric circulation. Dust emission was negatively correlated with precipitation and the surface temperatures except for the eastern deserts in China.
3) The WP and ACI indexes displayed a meridional and zonal correlation pattern for Asian dust aerosol and loading. AIAPV and IIAPV were strongly correlated with a zonal distribution of dust loading and deposition in the midlatitudes over the Asian subcontinent and North Pacific. The PNA and SOI displayed the opposite patterns of dust loading and deposition in the eastern Pacific, while SOI was correlated significantly with dust loading over eastern China and northeast Asia. The PDO affected the variation of dust aerosol not only in North America but also in the Asian dust sources.
4) For most regions, the variations of dust column loading and deposition have the same sign. Asian dust transport along the westerly jet forms the major loading pattern with the centers to the south side of the jets and the deposition pattern to the north side of the westerly jet.

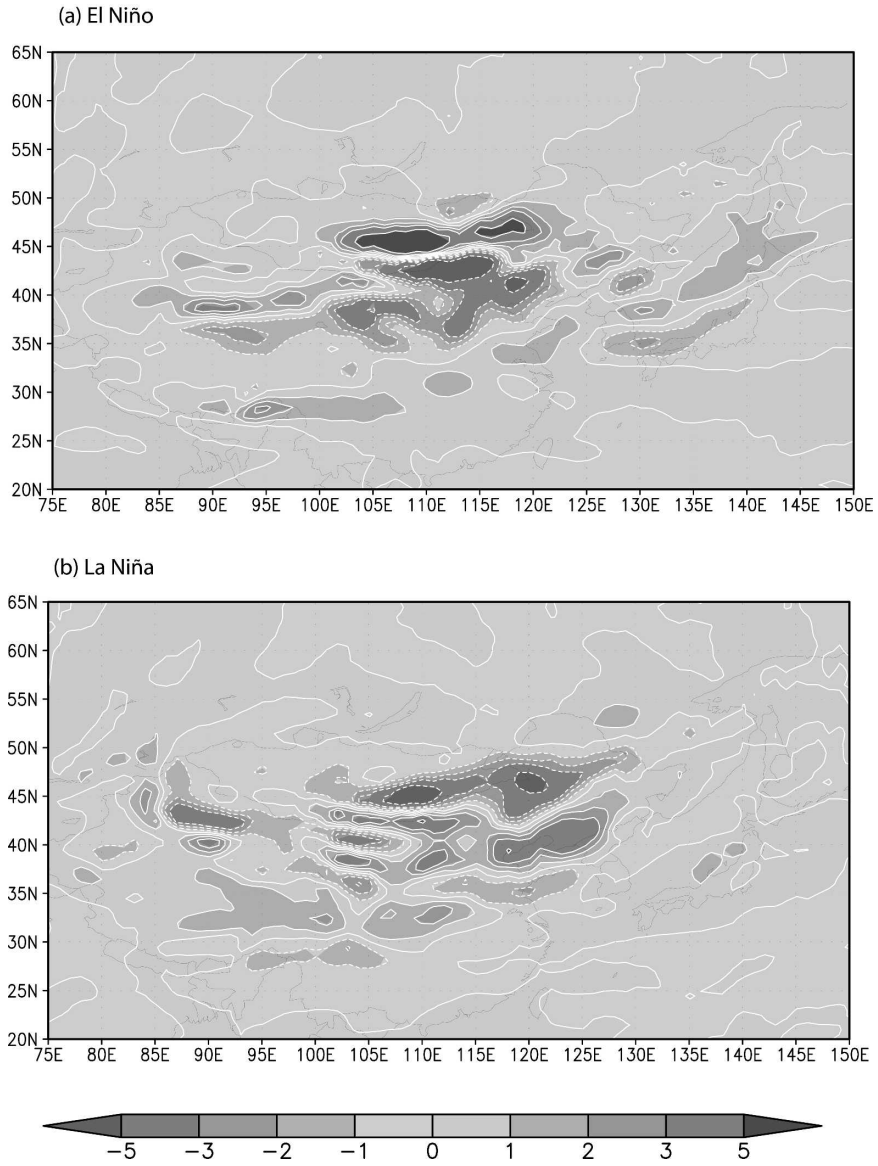

FIG. 10. Same as in Fig. 9, but between 3 and 10 km.

5) The anomalies of the dust loading for eight typical El Niño and eight La Niña years from the 44-yr-averaged values showed contrasting situations in most parts of China with a sharp negative anomaly for El Niño years and a positive anomaly for La Niña years. During El Niño years, the center of the trans-Pacific transport is 45°N, while during La Niña years it is around 40°N. The anomalies of dust trans-

TABLE 5. Correlations of Asian dust aerosol depositions and ratio of inflow to North America and outflow from the Asian continent with the climate indices.

Region		EAMI	WP	PDO	IIAPV	AIAPV	AO	SOI	PNA	ACI
Asian subcontinent depositions	Deserts	−0.085	−0.025	−0.235	0.465	0.295	*−0.190*	0.158		
	Nondeserts	0.209	0.044	−0.201	0.452	0.389	0.173	0.209		
North Pacific deposition		0.044	*−0.250*	−0.190	0.452	0.349		0.032	0.040	0.407
Ratio of inflow to NA and outflow over North Pacific		−0.118	0.294	−0.229	−0.090	−0.329		−0.485	*−0.555*	−0.340

port flux divergence reversed between El Niño and La Niña years in most regions of East Asia.

6) The relative amount of dust aerosols that reach the North American continent to the amount of dust exported from Asia is positively correlated with WP and negatively correlated with PNA. A positive PDO is associated with less dust deposition in the East Asian subcontinent and the North Pacific as well as reduced Asian dust transport to North America.

The global climate and atmospheric circulation is known to exhibit substantial variability. Obviously all the above discussed indices reflecting an important part of the interannual or interdecadal variability of the global climate and atmospheric circulation are interrelated in a system of global climate. Therefore, it is necessary to generally examine the connections of all major indices to variability of Asian dust. Their relationships with the interannual variability of Asian dust production, deposition, loading, and transport have been revealed here. The polar cold air outbreak, represented by the intensity and area index of Asian polar vortex (IIAPV and AIAPV), drives Asian dust production. The East Asian monsoon as one of the major components of global climate and has significant implications for Asian dust outflow from the Asian subcontinent and dust loading in the eastern Pacific and North America. Teleconnection patterns (WP and PNA) as well the zonal Atmospheric Circulation index (ACI) reflect large-scale changes in the atmospheric wave and westerly jet patterns over the North Pacific and influence the Asian dust aerosol and deposition over vast areas. El Niño and La Niña, the two opposite phases of the ENSO cycle, are critical in affecting the dust loading and the transport pathways across the Pacific. The Southern Oscillation index (SOI) exercises an influence on the dust aerosol and deposition in the extratropical regions, while the Pacific decadal oscillation (PDO), as result of air–sea interaction in the North Pacific, is directly related to dust aerosol and deposition in the midlatitude areas.

Finally, the relationships between major climate indices and dust production, transport, and deposition described herein suggest that there is considerable scope not only for improved forecasting of dust production and transport on a range of time scales, but also for improved understanding of the potential impacts and linkages associated with the transport of dust aerosol to remote areas (such as the North Pacific).

Acknowledgments. The authors wish to thank the Canadian Foundation for Climate and Atmospheric Sciences (CFCAS) for their partial financial support of this research. The authors also wish to thank the funds from MOST (G2000048703), the Aerosol and Climate Projects of CMA, NSF of China (90102017 and 49825105), and CAS (KZCX2-305) for their support.

REFERENCES

Alfaro, S. C., and L. Gomes, 2001: Modeling mineral aerosol production by wind erosion: Emission intensities and aerosol size distribution in source areas. *J. Geophys. Res.,* **106,** 18 075–18 084.

——, A. Gaudichet, L. Gomes, and M. Maillé, 1997: Modeling the size distribution of a soil aerosol produced by sandblasting. *J. Geophys. Res.,* **102,** 11 239–11 249.

An, Z. S., and S. C. Porter, 1997: Millennial-scale climatic oscillations during the last interglaciation in central China. *Geology,* **25,** 603–606.

——, T. S. Liu, Y. C. Lu, S. C. Porter, G. Kukla, X. H. Wu, and Y. M. Hua, 1990: The long-term paleomonsoon variation recorded by the loess-palaeosol sequence in central China. *Quat. Int.,* **718,** 91–95.

——, J. E. Kutzbach, W. L. Prell, and S. C. Porter, 2001: Evolution of Asian monsoons and phased uplift of the Himalaya-Tibetan plateau since late Miocene times. *Nature,* **411,** 62–66.

Barnston A. G., and R. E. Livezey, 1987: RPCA. *Mon. Wea. Rev.,* **115,** 1083–1126.

Cayan, D. R., M. D. Dettinger, H. F. Diaz, and N. E. Graham, 1998: Decadal variability of precipitation over western North America. *J. Climate,* **11,** 3148–3165.

——, K. T. Redmond, and L. G. Riddle, 1999: ENSO and hydrologic extremes in the western United States. *J. Climate,* **12,** 2881–2893.

Chen, L. X., W. Li, and P. Zhao, 2001: Impact of winter thermal condition of the Tibetan Plateau on the zonal wind anomaly over equatorial Pacific. *Sci. China,* **44D,** 400–410.

Chun, Y., K.-O. Boo, J. Kim, S.-U. Park, and M. Lee, 2001: Synopsis, transport and physical characteristics of Asian dust in Korea. *J. Geophys. Res.,* **106,** 18 461–18 469.

Ding, Y. H., 1994: *Monsoons over China*. Kluwer Academic, 419 pp.

Gong, S. L., X. Y. Zhang, T. L. Zhao, I. G. McKendry, D. A. Jaffe, and N. M. Lu, 2003a: Characterization of soil dust distributions in China and its transport during ACE-ASIA 2. Model simulation and validation. *J. Geophys. Res.,* **108,** 4262, doi:10.1029/2002JD002633.

——, and Coauthors, 2003b: Canadian Aerosol Module: A size-segregated simulation of atmospheric aerosol processes for climate and air quality models 1. Module development. *J. Geophys. Res.,* **108,** 4007, doi:10.1029/2001JD002002.

Guo, Q.-Y., 1988: An analysis of East Asian monsoon index and its variation (in Chinese). *Acta Geogr. Sin.,* **38,** 207–217.

Huang, R., and W. Li, 1988: Influence of heat source anomaly over the western tropical Pacific on the subtropical high over East Asia and its physical mechanism. *Sci. Atmos. Sin.,* Special Issue, 107–116.

Kang, I., and Y. Jeong, 1996: Association of interannual variations of temperature and precipitation in Seoul with principal modes of Pacific SST. *J. Korean Meteor. Soc.,* **32,** 339–345.

King, J. R., V. V. Ivanov, V. Kurashov, R. J. Beamish, and G. A. McFarlane, 1998: General circulation of the atmosphere over

the North Pacific and its relationship to the Aleutian Low. North Pacific Anadromous Fish Doc. No. 318, 18 pp.

Lau, K. M. and S. Yang, 1994: The influence of the Asian monsoon on the predictability of the tropical coupled ocean-atmosphere system. *Conf. on Monsoon Variability,* Triest, Italy, WCRP, WCRP-84, WMO/TD-619, 105–111.

Li, C., S. Sun, and M. Mu, 2001: Origin of the TBO-interaction between anomalous East-Asian winter monsoon and ENSO cycle. *Adv. Atmos. Sci.,* **18,** 554–566.

Li, W., and P. Zhai, 2003: Variability in occurrences of China's spring sand/dust storm and its relationship with atmospheric general circulation. *Acta Meteor. Sin.,* **17,** 396–405.

Liu, T. S., 1985: *Loess and the Environment*. China Ocean Press, 206 pp.

Mahowald, N., C. Luo, J. d. Corral, and C. S. Zender, 2003: Interannual variability in atmospheric mineral from a 22-year model simulation and observational. *J. Geophys. Res.,* **108,** 4352, doi:10.1029/2002JD002821.

Mantua, N. J., 1999: The Pacific decadal oscillation and climate forecasting for North America. *Climate Risk Solutions,* Vol. 1, No. 1, 10–13.

——, S. R. Hare, Y. Zhang, J. M. Wallace, and R. C. Francis, 1997: A Pacific interdecadal climate oscillation with impacts on salmon production. *Bull. Amer. Meteor. Soc.,* **78,** 1069–1079.

Marticorena, B., and G. Bergametti, 1995: Modeling the atmospheric dust cycle. Part 1: Design of a soil-derived dust emission scheme. *J. Geophys. Res.,* **100,** 16 415–16 430.

Merrill, J. T., M. Uematsu, and R. Bleck, 1989: Meteorological analysis of long-range transport of mineral aerosol over the North Pacific. *J. Geophys. Res.,* **94,** 8584–8598.

Natsagdorj, L., D. Jugder, and Y. S. Chung, 2003: Analysis of dust storms observed in Mongolia during 1937–1999. *Atmos. Environ.,* **37,** 1401–1411.

Nitta, T. S., 1986: Long-term variations of cloud amount in the western Pacific region. *J. Meteor. Soc. Japan,* **64,** 373–390.

Porter, S. C., and Z. S. An, 1995: Correlation between climate events in the North Atlantic and China during the last glaciation. *Nature,* **375,** 305–308.

Qian, W., L. Quan, and S. Shi, 2002: Variability of the dust storm in China and climatic control. *J. Climate,* **15,** 1216–1229.

Ramage, C. S., 1971: *Monsoon Meteorology*. Academic Press, 296 pp.

Shi, N., Q. Zhu, and B. Wu, 1996: The East-Asian summer monsoon in relation to summer large scale weather-climate anomaly in China for last 40 year. *J. Atmos. Sci. (China),* **20,** 385–394.

Tao, S., and Q. Zhang, 1998: Response of the East Asian summer monsoon to ENSO events (in Chinese). *Sci. Atmos. Sin.,* **22,** 399–407.

Thompson, D. W. J., and J. M. Wallance, 1998: The Arctic Oscillation signature in the winter geopotential height and temperature fields. *Geophys. Res. Lett.,* **25,** 1297–1300.

Tomita, T., and T. Yasunari, 1996: Role of the East Asian northeast winter monsoon on the biennial oscillation of the ENSO/monsoon system. *J. Meteor. Soc. Japan,* **74,** 399–413.

Wallace, J. M., and D. S. Gutzler, 1981: Teleconnections in the geopotential height field during the Northern Hemisphere winter. *Mon. Wea. Rev.,* **109,** 784–812.

Wang, B., R. Wu, and X. Fu, 2000: Pacific–East Asian teleconnection: How does ENSO affect East Asian climate? *J. Climate,* **13,** 1517–1536.

Webster, P. J., 1987: The variable and interactive monsoon. *Monsoons,* J. S. Fein and P. L. Stephens, Eds., Wiley-Interscience, 269–330.

——, and S. Yang, 1992: Monsoon and ENSO: Selectively interactive systems. *Quart. J. Roy. Meteor. Soc.,* **118,** 877–926.

——, V. O. Magana, T. N. Palmer, T. A. Tomas, M. Yanai, and T. Yasunari, 1998: Monsoons: Processes, predictability and prospects for prediction. *J. Geophys. Res.,* **103,** 14 451–14 510.

Wolter, K., and M. S. Timlin, 1998: Measuring the strength of ENSO—How does 1997/98 rank? *Weather,* **53,** 315–324.

Yasunari, T., and Y. Seki, 1992: Role of the Asian Monsoon on the interannual variability of the global climate system. *J. Meteor. Soc. Japan,* **70,** 177–189.

Zhang, X. Y., Z. S. An, and J. J. Cao, 1997: Dust emission from Chinese desert sources linked to variations in atmospheric circulation. *J. Geophys. Res.,* **102,** 28 041–28 047.

——, R. Arimoto, and Z. S. An, 1999: Glacial and interglacial patterns for Asian dust transport. *Quat. Sci. Rev.,* **18,** 811–819.

——, H. Y. Lu, R. Arimoto, and S. L. Gong, 2002: Atmospheric dust loadings and their relationship to rapid oscillations of the Asian winter monsoon climate: Two 250-kyr loess records. *Earth Planet. Sci. Lett.,* **202,** 637–643.

——, S. L. Gong, T. L. Zhao, R. Arimoto, and Y. Q. Wang, 2003: Sources of Asian dust and role of climate change versus desertification in Asian dust emission. *Geophys. Res. Lett.,* **30,** 2272, doi:10.1029/2003GL018206.

Zhang, Y., J. M. Wallace, and D. S. Battisti, 1997: ENSO-like interdecadal variability: 1900–93. *J. Climate,* **10,** 1004–1020.

Zhao, C., X. Dabu, and Y. Li, 2004: Relationship between climatic factors and dust storm frequency in the Inner Mongolia of China. *Geophys. Res. Lett.,* **31,** L01103, doi:10.1029/2003GL018206.

Zhao, T. L., S. L. Gong, X. Y. Zhang, and I. G. Mckendry, 2003: Modeled size segregated wet and dry deposition budgets of soil dust aerosol during ACE-Asia 2001: Implications for trans-Pacific transport. *J. Geophys. Res.,* **108,** 8665, doi:10.1029/2002JD003363.

——, ——, ——, J.-P. Blanchet, I. G. McKendry, and Z. J. Zhou, 2006: A simulated climatology of Asian dust aerosol and its trans-Pacific transport. Part I: Mean climate and validation. *J. Climate,* **19,** 88–103.

Zhong, D. C., 1999: The dynamic changes and trends of modern desert in China (in Chinese). *Adv. Earth Sci.,* **14,** 229–234.

Zhou, Z. J., and G. C. Zhang, 2003: Typical severe dust storms in northern China during 1954–2002. *Chinese Sci. Bull.,* **48,** 2366–2370.

Zhu, J. F., and Z. D. Zhu, 1999: *Combating Desertification in China*. Chinese Forest Press, 70 pp.